Exploring the Methanol Extract of *Persicaria Hydropiper* Leaves: Flavonoid Content, Antioxidant and Anti-inflammatory Potential, and Topical Gel Development for Wound Healing

Tabrej Mujawar[1], Sadaf Hashmi[2], Devlina Pal[3*], Rashmi Mohapatra[4], Jerin Murie Prabhu Das[5], Sandeep Nikam[6], Swapna.S[7], Tasneem Mohammed[8]

[1]*Department of Pharmacology, Gangamai College of Pharmacy, Nagaon Dhule MS India Pin- 424005.*
[2]*Axis Institute of Pharmacy, Kanpur, U.P India Pin 208001.*
[3]*Department of Pharmaceutical Technology, JIS University, 81, Nilgunj Road, Jagrata Pally, Deshpriya Nagar, Agarpara, Pin- 700109.*
[4]*Department of Botany and Head, Centre for Herbal Medicine and Therapeutics*
Kalinga Institute of Social Sciences (KISS), Deemed to be University
Bhubaneswar 751024 Odisha, India.
[5]*Department of Medicine, Caucasus University, Paata Saakadze St, Tbilisi 0102, Georgia, Pin code- 0102.*
[6]*Department of Pharmaceutics, Bharati Vidyapeeth's College of Pharmacy, Navi Mumbai – 400614.*
[7]*Department of Pharmaceutics, School of Pharmacy, Anurag University, Jodimetla, Ghatkesar-500088.*
[8]*Department of General Sciences, Ibn Sina National College for Medical Studies, Jeddah, KSA Pin – 21418.*
Corresponding Author: Devlina Pal[3]*

KEYWORDS
Persicaria hydropiper, Flavonoid content, Antioxidant activity, Anti-inflammatory effects, Lipid peroxide inhibition

ABSTRACT:
The present study aimed to develop and evaluate herbal gel formulations incorporating the methanol extract of *Persicaria hydropiper* leaves (PHLE-MA) for potential therapeutic applications. Six formulations (WGF1 to WGF6) were prepared using Carbopol 934 as the gelling agent, with varying concentrations of PHLE-MA (0.6–3.6%). The gels were characterized for pH, viscosity, spreadability, net content, extrudability, and physical appearance. In vitro diffusion studies revealed a concentration-dependent release of active constituents, with higher concentrations providing sustained release. Kinetic modeling of the release data showed that most formulations adhered to the Zero Order model, indicating controlled and consistent drug release, while others followed First Order or Higuchi Diffusion mechanisms. PHLE-MA demonstrated significant lipid peroxidation inhibition in egg yolk and liver homogenate models, showcasing its strong antioxidant activity. Additionally, COX-1 and COX-2 inhibition studies highlighted its anti-inflammatory potential, with IC50 values of 180.271 µg/mL and 188.361 µg/mL, respectively. The total flavonoid content of PHLE-MA was quantified as 321.44 mg/g quercetin equivalent. These findings underline the potential of PHLE-MA-based gel formulations as effective topical agents with antioxidant and anti-inflammatory properties, paving the way for their use in managing oxidative stress and inflammation-related conditions.

1. Introduction

Oxidative stress and inflammation are interconnected pathological processes implicated in the progression of numerous chronic diseases. Oxidative stress arises when there is an imbalance between reactive oxygen species (ROS) production and the body's antioxidant defense mechanisms. Excessive ROS can damage cellular components, including lipids, proteins, and DNA, leading to impaired cell function and tissue damage. This oxidative damage not only exacerbates existing conditions but also serves as a trigger for inflammatory responses (Hendrix et al., 2020, Sreejayan and Rao, 1997, Li et al., 2015). Inflammation is the body's natural defense mechanism against injury or infection, characterized by the activation of immune cells and the release of inflammatory mediators such as cytokines and prostaglandins. While acute inflammation is protective and resolves after the elimination of the harmful stimulus, chronic inflammation can persist and lead to tissue damage and fibrosis. Oxidative stress plays a pivotal role in the perpetuation of chronic inflammation by activating transcription factors like NF-κB, which regulate the expression of pro-inflammatory genes (Soga et al., 2012, Hendrix et al., 2020, Re et al., 1998, Packer, 2001, Kataki et al., 2012).

Conversely, inflammation exacerbates oxidative stress by stimulating ROS production through activated immune cells. This creates a vicious cycle that contributes to the pathogenesis of diseases such as cardiovascular disorders, diabetes, neurodegenerative diseases, and cancer. Targeting both oxidative stress and inflammation using antioxidants and anti-inflammatory agents is, therefore, a critical therapeutic strategy for managing these conditions effectively (Hendrix et al., 2020, Kakoti et al., 2015). Oxidative stress and inflammation play pivotal roles in the wound-healing process, influencing the progression and outcome of tissue repair. Wound healing is a complex, multi-phase process involving hemostasis, inflammation, proliferation, and remodeling. During the inflammatory phase, reactive oxygen species (ROS) are generated by activated immune cells such as neutrophils and macrophages as part of the defense mechanism against pathogens. While moderate ROS levels are essential for cellular signaling and immune defense, excessive ROS can lead to oxidative stress, damaging lipids, proteins, and DNA. This oxidative damage can impair cell migration, proliferation, and angiogenesis, thereby delaying wound healing (Li et al., 2003, Wu et al., 2007, Soga et al., 2012).

Inflammation, a critical phase in wound healing, ensures the recruitment of immune cells to the injury site to eliminate debris and pathogens. However, prolonged or chronic inflammation, often exacerbated by oxidative stress, can result in excessive tissue degradation and fibrosis, hindering proper healing (Ruch et al., 1989, Ahmad et al., 2016, D'Abrosca et al., 2019). The overproduction of pro-inflammatory cytokines and enzymes like COX-2 further contributes to this cycle, amplifying oxidative damage and delaying tissue repair. Effective wound healing requires a balance between ROS production and antioxidant defenses, as well as controlled inflammation. Natural compounds with antioxidant and anti-inflammatory properties, such as flavonoids and phenolic compounds, can mitigate oxidative stress and modulate inflammation. This dual action supports cellular regeneration and accelerates wound closure, emphasizing the importance of managing oxidative stress and inflammation in therapeutic strategies for wound care (Kakoti et al., 2015, Kataki et al., 2017).

Persicaria hydropiper (L.) Delarbre, a member of the Polygonaceae family, is a widely recognized medicinal plant with a rich history of traditional use. It is also known by several synonyms, including *Persicaria hydropiper var. projectum* Stanford, *Polygonum hydropiper* L., *Persicaria hydropiper* (L.) H. Gross, and *Persicaria hydropiper* (L.) Opiz. This plant is commonly referred to as marsh-pepper smartweed, marsh-pepper knotweed, smartweed, or water pepper in English (Khare, 2008). Regionally, it is known as pakarmul or bishkatali in Bangladesh, daun senahun in Malaysia, and la liao in China, reflecting its widespread cultural significance (Khare, 2008). Geographically, *P. hydropiper* is native to tropical and temperate regions of Asia, including the Caucasus, Western Asia, Middle Asia, Siberia, the Russian Far East, Eastern Asia, China, Indo-China, the Indian subcontinent, and Malesia. Its presence extends to Australia and Northern Africa as well. The plant predominantly thrives in moist environments such as marshes and areas near water bodies, often dominating agricultural fields (Khare, 2008).

The current study aims to explore the pharmacological potential of a microwave-assisted methanol extract derived from the leaves of *Persicaria hydropiper*. The study also aims to fabricate a topical herbal gel formulation of the extract. This historically valued medicinal plant will be assessed in various models to evaluate its effects on oxidative stress and inflammation, building upon its traditional applications and previous findings. This investigation seeks to expand the understanding of its therapeutic applications and contribute to its potential integration into modern medicinal practices (Huq et al., 2014).

2. Material and Methods

Chemicals, Reagents and Drugs

Quercetin and cyclophosphamide were generously provided as gift samples by Signova Pharmaceuticals Pvt. Ltd. Sodium Nitroprusside Griess Reagent, Thiobarbituric Acid, Sodium Dodecyl Sulfate, Tris-KCl Buffer, DTNB solution (Ellman's reagent), disodium edetate, and triethanolamine were obtained from Himedia Biosciences Company, Maharashtra, India. Trichloroacetic acid (TCA) and MTT reagent were sourced from Loba Chemie Pvt. Ltd., Maharashtra, India. Additionally, Carbopol 934, Carbopol 940, and propylene glycol were procured from Sigma-Aldrich, St. Louis, MO, USA. All other chemicals and reagents used in this study, acquired from verified vendors such as SRL Mumbai and E. Merck India, were of reagent grade and ensured high-quality standards.

Collection and identification (Plant Material)

The leaves of *Persicaria hydropiper* were carefully collected from their natural habitat between October 2021 and March 2022 to ensure the availability of mature and healthy plant material. The collection process was conducted with particular attention to preserving the plant's ecological surroundings. The collected specimens were subsequently authenticated and identified by Mr. A. Sharma, a local herbal practitioner associated with Angelica Herbs, Himachal Pradesh, India. The authentication process involved meticulous comparison with voucher specimens housed at the Department of Pharmacognosy Herbarium. This rigorous identification ensured the accurate taxonomical classification of the plant material used for the study.

Microwave assisted extraction of the extract

The collected leaves of *Persicaria hydropiper* were thoroughly cleaned to remove impurities such as dust and debris. The cleaned leaves were then shade-dried to preserve their phytochemical integrity and prevent degradation due to exposure to direct sunlight. Once dried, the leaves were pulverized into a fine powder using a motorized crusher, ensuring a consistent particle size for efficient extraction. The extraction process employed a microwave-assisted technique, as described by Mandal et al. (2007) (Mandal et al., 2007). A measured quantity of the powdered leaves (10 grams) was mixed with 100 ml of methanol in a solvent-to-powder ratio of 10:1. The mixture was subjected to microwave irradiation at a power setting of 170 W. The extraction process consisted of an initial microwaving period of five minutes, during which the mixture reached the desired temperature for optimal extraction. The temperature was then allowed to cool to room temperature before initiating a subsequent one-minute microwave cycle to ensure complete extraction of the bioactive compounds. The resulting extract was filtered to remove plant debris and particulate matter. The filtrate was then concentrated using an aqua bath to evaporate the solvent, yielding a dense and potent extract. This final extract was designated as PHLE-MA, standing for Microwave-Assisted Extract of *Persicaria hydropiper* leaves, and stored appropriately for further analysis and experimentation.

Determination of total flavanoid content

The flavonoid content in the microwave-assisted extract of *Persicaria hydropiper* leaves (PHLE-MA) was determined using a spectrophotometric method adapted from Ghasemi et al. (2009) (Ghasemi et al., 2009). This technique involved the use of aluminum chloride ($AlCl_3$), which forms complexes with flavonoids, resulting in a measurable absorbance peak at a specific wavelength. The flavonoid concentration was expressed as milligrams of quercetin equivalents per gram of plant extract (mg QE/g). To prepare the sample for analysis, 1 mL of PHLE-MA solution (1 mg/mL) was mixed with an equal volume (1 mL) of 2% methanolic $AlCl_3$ solution in a test tube. This mixture was vortexed briefly to ensure uniformity and then incubated at room temperature for 60 minutes to allow the reaction between flavonoids and $AlCl_3$ to reach completion. Following incubation, the absorbance of the solution was measured at 415 nm using a Shimadzu UV-1800 spectrophotometer. The wavelength of 415 nm was selected as it corresponds to the maximum absorbance of the $AlCl_3$-flavonoid complex,

ensuring precise detection. To ensure accuracy and reproducibility, each sample was prepared and analyzed in triplicate. The mean absorbance values from these measurements were used for further calculations. A standard curve was also prepared using a series of quercetin solutions of known concentrations, following the same procedure. The absorbance values of these standards were plotted against their respective concentrations to create a calibration curve, which served as a reference for determining the flavonoid content in the extract. The flavonoid content of PHLE-MA was calculated by interpolating the sample's absorbance on the quercetin standard curve. The final results were expressed as the equivalent milligrams of quercetin per gram of plant extract (mg QE/g), providing a quantitative measure of the extract's flavonoid concentration. This method is widely recognized for its reliability and precision in quantifying flavonoids in plant-based samples.

Inhibition of lipid peroxidation using egg yolk

The lipid peroxide product produced was measured using a modified thiobarbituric acid reactive species (TBARS) assay with egg yolk as a lipid-rich medium (Badmus et al., 2011). The inhibition of lipid peroxidation was assessed using egg yolk as a lipid-rich medium, employing a modified thiobarbituric acid reactive species (TBARS) assay as described by Badmus et al. (2011). This method evaluates the ability of the extract to prevent lipid peroxidation by measuring the formation of malondialdehyde (MDA), a key lipid peroxide product, through its reaction with thiobarbituric acid (TBA). To prepare the reaction mixture, 0.4 mL of the extract at varying concentrations (15–180 µg/mL) was mixed with 0.8 mL of 15% (v/v) egg yolk emulsion, which served as a lipid substrate. To this, 1.5 mL of distilled water was added to ensure the reaction volume was consistent. The mixture was then treated with 0.07 mL of freshly prepared ferrous sulfate ($FeSO_4$) solution to initiate lipid peroxidation. The reaction mixture was incubated for 30 minutes at 37°C, allowing sufficient time for oxidative degradation of lipids. Following incubation, 1.7 mL of TBA in sodium dodecyl sulfate (SDS) solution and 1.7 mL of acetic acid were added. The acidic medium facilitates the reaction of TBA with MDA, forming a pink chromogen that can be spectrophotometrically measured. The entire mixture was thoroughly mixed to ensure uniformity and subsequently heated at 96°C for one hour in a water bath. This heating step enhances the reaction between TBA and MDA. After cooling the mixture to room temperature, 5 mL of butanol was added to extract the TBA-MDA complex into the organic phase. The mixture was centrifuged at 5000 rpm for 11 minutes to separate the phases. The organic top layer, containing the TBA-MDA complex, was carefully collected, and its absorbance was measured at 532 nm using a UV-visible spectrophotometer.

$$\%\ \textbf{inhibition of lipid peroxidation} = \left(\frac{100 - A_{SAMPLE}}{A_{CONTROL}}\right) \times 100$$

Evaluating the Anti-inflammatory activity: Cycloxygenase–1 (COX–1) and cycloxygenase–2 (COX–2) assays

The COX-1 assay was carried out in accordance with the procedure detailed elsewhere (Redl et al., 1994, Aguilar et al., 2002). The cyclooxygenase (COX) inhibitory activity of the extract was evaluated using specific assays for COX-1 and COX-2 enzymes, following protocols described by Redl et al. (1994) and Aguilar et al. (2002). The COX-1 assay was performed to determine the extract's ability to inhibit COX-1, an enzyme crucial for producing prostaglandins involved in normal physiological functions. The assay began by preparing a reaction mixture containing 192 µL of 0.2 M Tris-HCl buffer (pH 7.4), 19 µL of L-adrenaline-D-hydrogentartrate as a reducing agent, 12 µL of hematin as a cofactor, and 12 µL of the sample solution. The enzymatic reaction was initiated by adding 0.3 U of COX-1 and incubating the mixture at 37°C for 6 minutes. Arachidonic acid (6 µL) was then added as a substrate, and the reaction continued for 30 minutes at 37°C. To stop the enzymatic activity, 12 µL of 12% formic acid was added. The prostaglandin E2 (PGE2) levels, a product of the COX pathway, were measured using a PGE2 enzyme immunoassay kit from R&D Systems. The COX-2 assay

followed a similar procedure to evaluate the extract's inhibitory effect on COX-2, an enzyme primarily associated with inflammation. The reaction mixture consisted of 192 µL of 0.2 M Tris-HCl buffer (pH 7.4), 19 µL of L-adrenaline-D-hydrogentartrate, 12 µL of sodium edetate (Na_2-EDTA) to chelate metal ions, 12 µL of hematin, and 12 µL of the sample solution. After adding 0.3 U of COX-2 enzyme, the mixture was pre-incubated at 37°C for 6 minutes. Arachidonic acid (6 µL) was then introduced as a substrate, and the reaction was allowed to proceed for 30 minutes at 37°C. The enzymatic activity was halted by adding 12 µL of 12% formic acid. The PGE2 levels produced in the COX-2 pathway were quantified using a PGE2 enzyme immunoassay kit from Cayman Systems (Redl et al., 1994, Aguilar et al., 2002). Both assays were conducted in triplicate to ensure reproducibility and accuracy. The percent inhibition of COX activity was calculated by comparing the PGE2 levels in the presence and absence of the extract. This approach provided a comprehensive assessment of the extract's inhibitory potential against COX-1 and COX-2 enzymes. The findings highlight the extract's ability to modulate prostaglandin synthesis and its promising potential as an anti-inflammatory agent for therapeutic applications.

Formulation Development: The Herbal Gel Formulation

Fabrication of the gel base

The gel base was prepared using a stepwise process to ensure homogeneity and prevent agglomeration. Initially, 1 g of Carbopol 934 was gradually dispersed in 70 mL of demineralized water with continuous stirring. The stirring was maintained for an hour to fully hydrate the polymer and achieve a uniform dispersion. This step was crucial to avoid the formation of clumps and ensure a smooth consistency of the gel base. Separately, disodium edetate (0.1 g) and triethanolamine (0.6 mL) were dissolved in 12 mL of demineralized water. The solution was stirred vigorously for 12 minutes to achieve complete dissolution of both components. These ingredients were selected for their roles as a chelating agent and a neutralizing agent, respectively, with triethanolamine also serving to adjust the pH of the gel base. In another beaker, 4.90 mL of propylene glycol was mixed with 15 mL of demineralized water and stirred for 13 minutes to form a homogenous solution. Propylene glycol was included as a humectant and a solvent to enhance the stability and hydration properties of the gel (Aiyalu et al., 2016a). The disodium edetate and triethanolamine solution was then slowly added to the Carbopol dispersion with continuous stirring. This step allowed the pH of the mixture to be raised to approximately 7.4, which is essential for achieving optimal gel consistency. The pH adjustment facilitated the neutralization of Carbopol, leading to the development of a clear and viscous gel matrix. Finally, the propylene glycol solution was added to the neutralized Carbopol gel. The mixture was stirred for an additional 12 minutes to ensure complete incorporation of all components and to achieve a uniform, transparent gel base. This systematic method resulted in a high-quality gel base suitable for further incorporation of active pharmaceutical ingredients.

Preparation of gel formulation

A total of twelve topical gel formulations were prepared following the drug formulation manual (Kohli and Shah, 1998). The herbal gel formulations (WGF1 to WGF6) were prepared using a standardized method to ensure uniformity and reproducibility. Initially, 1.6 g of Carbopol 934 was gradually dispersed in approximately 60 mL of demineralized (D.M.) water with continuous stirring using a mechanical stirrer. The dispersion was stirred for one hour to allow complete hydration of the polymer, ensuring a smooth and lump-free gel base. In parallel, a neutralizing solution was prepared by dissolving 1.6 g of triethanolamine and 0.006 g of disodium EDTA in 10 mL of D.M. water, which was stirred thoroughly for 10 minutes until completely dissolved. Another solution containing 6 g of propylene glycol in 12 mL of D.M. water was also prepared, ensuring homogeneity after stirring for 10 minutes. The active ingredient, methanol extract of *Persicaria hydropiper* (PHLE-MA), was weighed in varying amounts (0.6–3.6 g for WGF1 to WGF6, respectively) and dissolved in a small volume of D.M.

water. The extract solution was stirred thoroughly to ensure complete dissolution of the active constituents. The neutralizing solution was then added slowly to the hydrated Carbopol base under continuous stirring, raising the pH to approximately 7.4 to optimize viscosity and stability. The PHLE-MA solution was incorporated into the gel base with constant stirring, followed by the gradual addition of the propylene glycol solution. The entire mixture was stirred for an additional 10 minutes to ensure uniform distribution of all components. Finally, the total weight of the formulation was adjusted to 100 g with D.M. water, and the gel was stirred for another 5 minutes to achieve a smooth and homogenous texture. The completed formulations were carefully transferred into sterilized containers, labelled as WGF1 to WGF6, and stored at room temperature in a clean and dry environment for further characterization and evaluation. This method ensured the preparation of high-quality gels with consistent properties suitable for topical application.

Table 1. The composition stating the ingredients for the herbal gel formulations.

	Gel Formulation code					
Ingredients	**WGF1**	**WGF2**	**WGF3**	**WGF4**	**WGF5**	**WGF6**
PHLE-MA (g)	0.6	1.2	1.8	2.4	3	3.6
Carbopol 934 (g)	1.6	1.6	1.6	1.6	1.6	1.6
Triethanolamine (g)	1.6	1.6	1.6	1.6	1.6	1.6
Disodium EDTA (g)	0.006	0.006	0.006	0.006	0.006	0.006
Propylene Glycol (g)	6	6	6	6	6	6
D.M. water (100 g)	q.s	q.s	q.s	q.s	q.s	q.s

Characterization of the gel formulation

Assessment of active constituents

Each gel formulation was analyzed for active constituents using a standardized spectrophotometric method. A sample of 1 g of the gel was placed into a 50 mL volumetric flask, and methanol was added to dissolve the active ingredients. The flask was vigorously shaken to ensure complete dissolution of the constituents in the methanol. The solution was then filtered using Whatman filter paper to remove any insoluble residues. An aliquot of 0.1 mL of the filtrate was carefully measured and diluted to a final volume of 10 mL with methanol to prepare a test solution suitable for analysis. The concentration of the active constituents in this solution was determined using UV spectrophotometry at 280 nm, the wavelength corresponding to the maximum absorbance (λmax) of the active compounds. A standard curve was constructed by analyzing standard solutions of known concentrations, and the absorbance values of the test solutions were interpolated against this curve to quantify the active constituents. This method ensured accurate and reliable determination of the active components in the gel formulation (Nandgude et al., 2008).

Extrudability

The extrudability of the gel formulation was assessed to evaluate its ease of extrusion from the container, which is an important parameter for user convenience. A collapsible aluminum or plastic tube containing the gel was placed between two glass slides, and a standard weight (e.g., 500 g) was applied over the top slide. The amount of gel extruded in 10 seconds was collected and weighed. The extrudability was expressed in terms of the quantity of gel extruded per unit weight applied. This test ensured that the gel had optimal consistency for smooth and effortless dispensing without being too runny or too viscous (Aiyalu et al., 2016b).

Measurement of the pH

The pH of the gel formulation was determined to ensure compatibility with the skin's natural pH and to minimize irritation upon application. A small quantity of gel (1 g) was dispersed in 10 mL of demineralized water to form a uniform solution. The pH was measured using a calibrated digital pH meter, with the electrode immersed in the gel dispersion. The pH was adjusted during the formulation process to a value close to 7.4, ensuring it remained within the

acceptable range (typically 6.8–7.5) for topical applications. Regular checks were conducted to ensure the pH stability of the gel during storage (Queiroz et al., 2009).

Appearance, homogeneity and viscosity

Appearance

The appearance of the gel formulation was visually inspected to evaluate its color, clarity, and overall aesthetic quality. A uniform and smooth texture without any visible particles, phase separation, or air bubbles was considered an indicator of a well-formulated gel. The gel was checked for consistency in color and transparency (if applicable) across batches, ensuring that it met the desired quality standards for topical application (Nayak et al., 2005).

Homogeneity

The homogeneity of the gel was assessed by spreading a small amount of the formulation on a clean glass slide and examining it under a light source. The gel was checked for the presence of any lumps, clumps, or particulate matter. A smooth and uniform distribution of the constituents indicated proper mixing and effective formulation of the gel (Nayak et al., 2005).

Viscosity

The viscosity of the gel formulation was measured using a Brookfield viscometer to evaluate its rheological properties. The gel was loaded onto the viscometer, and the spindle (appropriate for semi-solid formulations) was rotated at various speeds (rpm) at room temperature. The viscosity values were recorded at each speed to determine the flow behavior of the gel. An ideal gel exhibits pseudo-plastic or shear-thinning behavior, which ensures ease of application and spreadability while maintaining stability during storage. These viscosity measurements were critical in optimizing the gel's consistency for effective topical use (Nayak et al., 2005).

Spreadibility

Spreadability is a critical parameter that determines the ease with which the gel can be applied uniformly over the skin. It directly influences user satisfaction and the therapeutic efficacy of the formulation. The spreadability of the gel was evaluated using the slip and drag method.

In this method, a fixed amount of gel (e.g., 1 g) was placed between two clean glass plates. A standard weight (e.g., 500 g) was applied to the top plate for a specified time (usually one minute) to allow the gel to spread. The diameter or area covered by the gel after the weight was removed was measured. The spreadability was calculated using the formula:

$S = M \times L / T$

where:

- S is the spreadability,
- M is the weight applied (in grams),
- L is the length of gel spread (in cm),
- T is the time taken (in seconds).

The gel formulation with higher spreadability values indicates easier and more uniform application on the skin surface. This test ensures that the gel can be evenly distributed without excessive effort, making it user-friendly and effective for topical delivery (Jain, 2007).

Diffusion study In vitro: permeation using rat skin

The in vitro diffusion study was conducted to evaluate the permeation potential of the gel formulation through rat skin, simulating transdermal delivery. Male Wistar rats (150–200 g) were used for the study, and their abdominal skin was carefully excised, ensuring no damage to the dermal layer. The skin was cleaned of subcutaneous tissue and fat, washed with saline, and stored at -20°C until use. Before the experiment, the skin was hydrated in phosphate buffer (pH 7.4) for one hour at room temperature. The study utilized a Franz diffusion cell with an effective diffusion area of 2.5 cm^2 and a receptor compartment volume of 15 mL. The hydrated rat skin was mounted between the donor and receptor compartments, with the stratum corneum facing the donor side and the dermis in contact with the receptor medium. Phosphate buffer (pH 7.4) served as the receptor medium, maintained at 37 ± 1°C with continuous stirring to mimic physiological conditions. A fixed amount of the gel formulation (approximately 1 g)

was evenly applied to the donor compartment. Samples (1 mL) were withdrawn from the receptor compartment at predetermined intervals (e.g., 0, 1, 2, 4, 6, 8, and 12 hours) and replaced with an equal volume of fresh phosphate buffer to maintain sink conditions. The collected samples were analyzed spectrophotometrically at 280 nm to quantify the active constituents permeated through the skin. The cumulative amount of drug permeated per unit area (µg/cm²) was plotted against time to generate the permeation profile. The steady-state flux (Jss) was calculated from the linear portion of the permeation curve, and the permeability coefficient (Kp) was determined by relating the flux to the concentration of the active ingredient in the donor compartment. This study provided valuable insights into the release and skin permeation characteristics of the gel formulation, helping to optimize its design for effective transdermal delivery and therapeutic efficacy. The use of rat skin as a model ensured a realistic evaluation of the gel's performance under controlled in vitro conditions (Jain, 2007).

Release Kinetics of Gel Formulation

The release kinetics of the active constituents from the gel formulation were studied to understand the mechanism of drug release and ensure controlled and sustained delivery. The study was conducted using an in vitro diffusion setup, typically a Franz diffusion cell, and the release profile was analyzed at regular time intervals (Martin et al., 2011). The release kinetics of the active constituents from the gel formulation were evaluated to understand the mechanism of drug release and ensure it met the criteria for controlled and sustained delivery. The study was conducted using an in vitro diffusion setup, typically a Franz diffusion cell, with phosphate buffer (pH 7.4) as the receptor medium maintained at 37 ± 1°C under continuous stirring. A specific amount of the gel formulation was applied to the donor compartment, and aliquots were withdrawn from the receptor medium at predetermined time intervals while maintaining sink conditions by replacing the withdrawn volume with fresh buffer. The collected samples were analyzed spectrophotometrically at 280 nm to quantify the active constituents released at each time point. The cumulative release data were plotted against time to generate a release profile, which was then fitted into various mathematical models to understand the release mechanism. These included the zero-order model, which assumes a constant release rate; the first-order model, which is concentration-dependent; the Higuchi model, which describes diffusion-based release; and the Korsmeyer-Peppas model, which provides insights into whether the release is governed by diffusion, erosion, or a combination of both. The model that best fit the data, as indicated by the highest correlation coefficient, was considered the most appropriate to describe the release kinetics. This analysis helped determine whether the gel formulation provided a sustained and predictable release pattern, ensuring its suitability for therapeutic applications. The insights gained from the release kinetics study were crucial for optimizing the formulation to achieve the desired drug delivery profile.

Statistical analysis

Statistical analysis was performed to validate the results obtained from various experiments and ensure their reliability and reproducibility. All experiments were conducted in triplicate, and the data were expressed as mean ± standard deviation (SD). This approach provided a measure of central tendency and variability, ensuring that the results were representative and consistent. To determine the significance of differences between groups or formulations, appropriate statistical tests were employed. For comparing multiple groups, one-way analysis of variance (ANOVA) was performed, followed by post hoc tests such as Tukey's test for pairwise comparisons. In cases where only two groups were compared, an independent t-test was applied. A p-value of less than 0.05 was considered statistically significant, indicating a meaningful difference between the compared groups. Regression analysis was used for fitting the release data into various kinetic models, and the goodness of fit was evaluated using the correlation coefficient (r^2). Higher r^2 values indicated better adherence to the respective models. All statistical analyses were carried out using specialized software such as GraphPad Prism (Version 8) to ensure accuracy and efficiency. This rigorous statistical approach validated the

experimental findings and provided a robust basis for interpreting the performance and efficacy of the gel formulations.

3. Results and Discussion

Total flavanoid content estimation

The total flavonoid content (TFC) of the methanol extract of *Persicaria hydropiper* leaves (PHLE-MA) was determined to be 321.44 mg/g of quercetin equivalent (QE). Using the calibration curve equation y = 0.0207x + 0.0992, R^2 = 0.9779 (R2=0.9779), the absorbance values obtained were used to quantify the flavonoid content. This significant amount of flavonoids highlights the extract's potential for antioxidant and therapeutic applications.

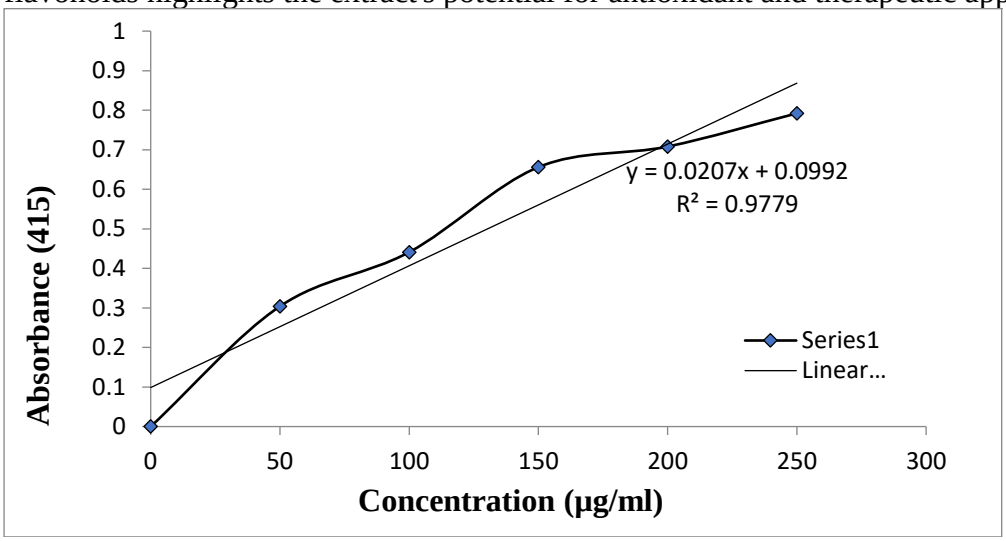

Figure 1. Standard curve of Quercetin for estimation of total flavanoid content in PHLE-MA.

Inhibition of Lipid peroxidation in egg yolk model

The percentage inhibition of lipid peroxidation by the methanol extract of *Persicaria hydropiper* leaves (PHLE-MA) was evaluated in the egg yolk homogenate model and compared with ascorbic acid as the standard. The results indicate a concentration-dependent inhibition of lipid peroxidation by PHLE-MA, with the highest inhibition of 77.73 ± 1.11% observed at 180 µg/mL, which was significantly close to that of ascorbic acid (89.02 ± 1.16%) at the same concentration. Similarly, at lower concentrations (90, 60, 30, and 15 µg/mL), PHLE-MA exhibited progressive reductions in inhibitory activity, with values of 68.70 ± 1.14%, 60.62 ± 1.17%, 49.46 ± 1.18%, and 37.50 ± 1.17%, respectively. Although the percentage inhibition was slightly lower than ascorbic acid at all tested concentrations, PHLE-MA demonstrated statistically significant inhibition ($p < 0.05$), confirming its potential as an effective antioxidant. These findings suggest that PHLE-MA contains bioactive compounds capable of reducing oxidative stress by inhibiting lipid peroxidation. The concentration-dependent activity underscores the dose-related efficacy of the extract, which could be attributed to the presence of flavonoids and other phenolic compounds with known antioxidant properties. While ascorbic acid exhibited superior activity across all concentrations, the comparable performance of PHLE-MA, particularly at higher concentrations, indicates its potential as a natural antioxidant. This activity further supports the traditional use of *P. hydropiper* in managing conditions associated with oxidative stress, highlighting its relevance for therapeutic and nutraceutical applications.

Table 2. Percentage lipid peroxidation inhibition of PHLE-MA in the egg yolk homogenates model

Media	Concentration (µg/ml)	PHLE-MA (%)	Ascorbic acid (%)
Egg yolk	180 µg/ml	77.73 ± 1.11*	89.02± 1.16*
	90 µg/ml	68.70 ± 1.14*	80.31 ± 1.77*
	60 µg/ml	60.62 ± 1.17*	74.51 ± 1.87*
	30 µg/ml	49.46 ± 1.18*	56.07 ± 1.90*
	15 µg/ml	37.50 ± 1.17*	50.11 ± 1.36

The mean of three replicate measurements plus the standard deviation (SD) is used to express values. Significant differences from ascorbic acid at *p < 0.05 and **p < 0.01.

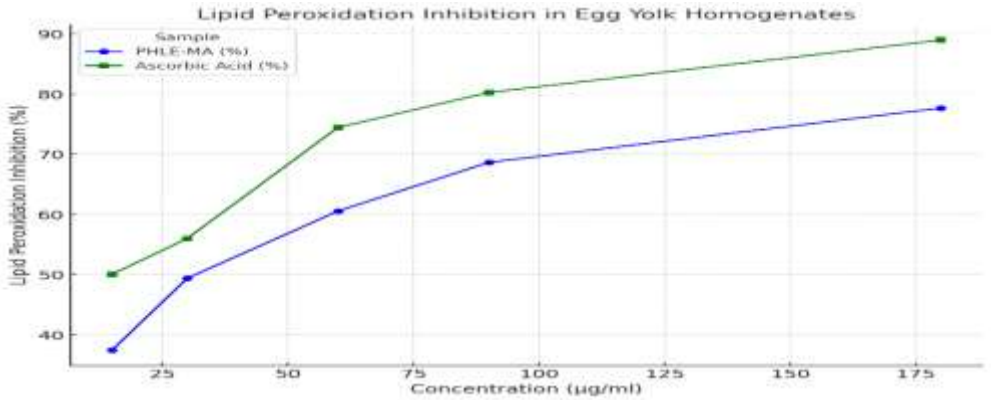

Figure 2. Lipid peroxidation inhibition percentage of PHLE-MA in the egg yolk homogenates model

Inhibition of Lipid peroxidation in liver homogenate model

The inhibition of lipid peroxidation (LPO) by the methanol extract of *Persicaria hydropiper* leaves (PHLE-MA) was assessed in vitro using a liver homogenate model and compared with catechin, a standard antioxidant. PHLE-MA demonstrated significant, concentration-dependent inhibition of LPO, with the highest activity observed at 180 µg/mL, where it inhibited 85.34 ± 1.08% of lipid peroxidation. Although slightly lower than catechin (93.28 ± 1.14%) at the same concentration, the difference was statistically significant (**p < 0.01). At lower concentrations, PHLE-MA exhibited a progressive reduction in inhibitory activity: 76.03 ± 1.08% at 90 µg/mL, 67.25 ± 1.06% at 60 µg/mL, 56.65 ± 1.04% at 30 µg/mL, and 45.02 ± 1.05% at 15 µg/mL. Comparatively, catechin displayed higher activity across all tested concentrations, with 89.13 ± 1.17% at 90 µg/mL, 78.16 ± 1.14% at 60 µg/mL, 64.71 ± 1.09% at 30 µg/mL, and 58.68 ± 1.03% at 15 µg/mL. While catechin showed superior antioxidant activity, the results for PHLE-MA were significant (*p < 0.05 and **p < 0.01) and demonstrated its efficacy as a natural antioxidant. The strong inhibition of lipid peroxidation by PHLE-MA in liver homogenates can be attributed to its high content of flavonoids and phenolic compounds, which are known to scavenge free radicals and prevent oxidative degradation of lipids. These findings validate the extract's potential in mitigating oxidative stress, particularly in liver-related oxidative damage, and support its therapeutic application in conditions where lipid peroxidation is implicated. The comparable performance of PHLE-MA to catechin highlights its promise as a natural alternative for managing oxidative stress.

Table 3. Inhibition of Lipid peroxidation (LPO) appraisal *in vitro* using liver homogenate ***p < 0.01*

Media	Concentration (µg/ml)	PHLE-MA (%)	Catechin (%)
Liver homogenate	180 µg/ml	85.34 ± 1.08**	93.28 ± 1.14**
	90 µg/ml	76.03 ± 1.08**	89.13 ± 1.17*
	60 µg/ml	67.25 ± 1.06*	78.16 ± 1.14*
	30 µg/ml	56.65 ± 1.04*	64.71 ± 1.09*
	15 µg/ml	45.02 ± 1.05*	58.68± 1.03*

The mean of three replicate measurements plus the standard deviation (SD) is used to express values. Significant differences from Catechin at *p < 0.05 and **p < 0.01.

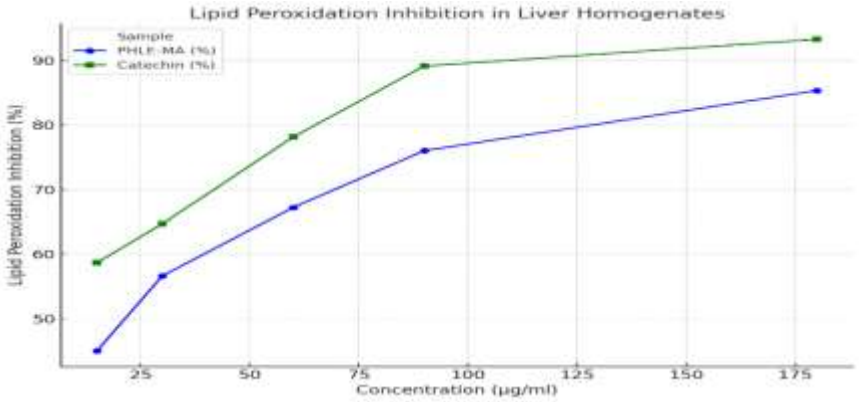

Figure 3. Inhibition of Lipid peroxidation (LPO) appraisal in vitro using liver homogenate

Anti-inflammatory activity

Measuring the Cyclooxygenase-1 (COX-1) and cyclooxygenase-2 (COX-2) assays

The percentage inhibition of COX-1 and COX-2 enzymes by the methanol extract of *Persicaria hydropiper* leaves (PHLE-MA) was evaluated at various concentrations (60–300 µg/mL). The results demonstrated a concentration-dependent inhibition of both COX-1 and COX-2 enzymes. At the highest concentration (300 µg/mL), PHLE-MA exhibited the most significant inhibitory activity, with 98.713 ± 0.84% inhibition of COX-1 and 90.475 ± 0.982% inhibition of COX-2, indicating potent anti-inflammatory properties. At lower concentrations, the inhibitory activity was comparatively modest but showed a clear dose-response relationship. For COX-1, the inhibition ranged from 4.831 ± 0.012% at 60 µg/mL to 49.102 ± 0.63% at 240 µg/mL. Similarly, COX-2 inhibition ranged from 6.783 ± 0.114% at 60 µg/mL to 48.872 ± 0.881% at 240 µg/mL. The IC50 values for COX-1 and COX-2 were 180.271 µg/mL and 188.361 µg/mL, respectively, indicating the concentration at which the extract inhibited 50% of the enzyme activity. These results highlight the dual inhibitory potential of PHLE-MA on both COX-1 and COX-2 enzymes, with a slightly higher efficacy for COX-1 at higher concentrations. This balanced inhibition suggests that PHLE-MA may have therapeutic potential in managing inflammatory conditions while minimizing adverse effects commonly associated with selective COX inhibition. The strong COX inhibition observed at higher concentrations can be attributed to the presence of bioactive compounds, such as flavonoids and phenolics, known for their anti-inflammatory properties. This study underscores the potential of PHLE-MA as a natural anti-inflammatory agent for further pharmacological development.

Table 4. Percentage enzyme inhibition of the COX system by the herbal blend (PHLE-MA).

	% Enzyme Inhibition	
Concentration (µg/mL)	**COX-1**	**COX-2**
60	4.831±0.012	6.783±0.114
120	9.171±0.434	14.225±0.478
180	26.115±0.21	31.661±0.689
240	49.102±0.63	48.872±0.881
300	98.713±0.84	90.475±0.982
IC_{50}	180.271 µg/mL	188.361 µg/mL

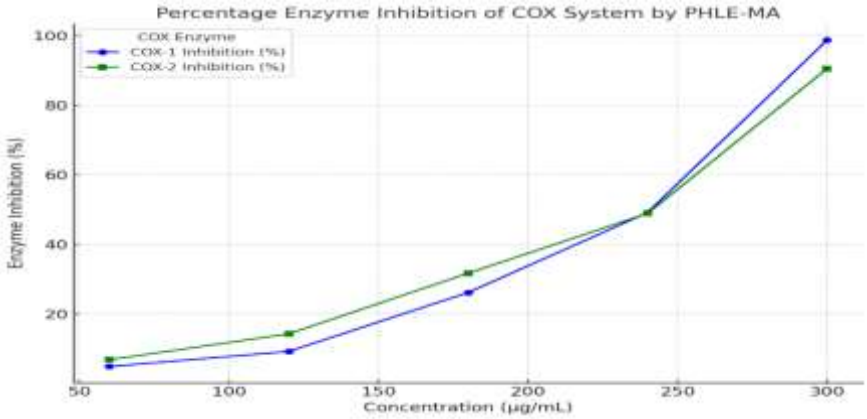

Figure 4. Percentage enzyme inhibition of the COX system by the herbal blend (PHLE-MA).

Herbal Gel Formulation development and evaluation of the topical herbal gel

Among various topical semisolid preparations, gel formulations are generally preferred for several reasons. They offer numerous advantages such as prolonged residence time on the skin, high viscosity, moisturizing effects for flaky skin due to their occlusive properties, enhanced bioadhesiveness, reduced irritation, independence from the water solubility of active ingredients, ease of application, and improved release characteristics (Loganathan et al., 2001, Oktay et al., 2020, Panigrahi et al., 2006). Numerous studies have highlighted the anti-inflammatory, antioxidant, protective and anti-aging activities of flavonoids, and phenolic compounds found in herbs. Moreover, these polyphenolic flavonoids have demonstrated the ability to penetrate the human skin (Ghasemzadeh and Ghasemzadeh, 2011, Ratz-Łyko et al., 2015, Stelmakienė et al., 2015, Seelinger et al., 2008). Based on these findings, a topical herbal gel formulation was developed to incorporate the extracts rich in flavonoid and phenolic compounds for the prevention and treatment of wound as well as inflammation and associated conditions (Blanco-Fuente et al., 1996, Walker and Smith, 1996, Murthy and Shivakumar, 2010).

Fabrication and Characterisation for the Formulated Topical Herbal Gel

The topical gel formulations (WGF1 to WGF6), prepared with Carbopol 934 at a 1.5% concentration, were characterized based on pH, viscosity, spreadability, net content, extrudability, and physical appearance. The results demonstrated consistent quality across all formulations, with slight variations attributed to the increasing concentration of the active extract. The pH values of the formulations ranged from 7.37 ± 1.09 to 7.71 ± 0.84, remaining close to skin-friendly levels, ensuring compatibility for topical application. The viscosity values were consistent across all formulations, ranging from 0.3897 ± 0.0027 to 0.3976 ± 0.0021 poise, indicating optimal gel consistency suitable for application and stability during storage. Spreadability, a key parameter for user convenience, increased with the concentration of the active extract. WGF1, containing the lowest extract concentration (0.6%), exhibited a spreadability of 31.12 ± 1.27 g cm/sec, while WGF6, with the highest concentration (3.6%),

showed a spreadability of 75.73 ± 1.31 g cm/sec. This trend highlights the improved ease of application with increasing extract concentration. The net content of the active ingredient ranged between 99.48 ± 1.79% and 102.55 ± 1.87%, indicating excellent uniformity in the distribution of the extract across all formulations. Extrudability was rated as "Good" for formulations WGF1 to WGF3 and "Excellent" for WGF4 to WGF6, reflecting an improved ease of dispensing with higher extract concentrations. All formulations appeared homogenous, translucent, and dark-greenish, confirming the successful incorporation of the extract without phase separation or particulate matter. These results indicate that the gels were well-formulated with optimal properties for effective and user-friendly topical application, with higher concentrations of the active extract enhancing specific characteristics such as spreadability and extrudability. This suggests the potential for tailoring the formulation to specific therapeutic needs while maintaining consistent quality.

Table 5. Characterizations for the topical gel formulations fabricated with Carbopol 934 at 1.5% concentration.

Code	**Conc (%)**	**pH**	**Viscosity (poise)**	**Spread ability (g cm/sec)**	**Net Content (% w/w)**	**Extrud ability**	**Physical Appearance**
WGF 1	0.6	7.47± 0.87	0.3976± 0.0021	31.12 ± 1.27	99.48± 1.79	Good	Homogeneous, translucent, dark-greenish
WGF 2	1.2	7.47± 0.88	0.3903± 0.0028	43.27 ± 1.22	101.86±2. 44	Good	Homogeneous, translucent, dark-greenish
WGF 3	1.8	7.71± 0.84	0.3908± 0.0033	54.51 ± 1.27	102.55± 1.87	Good	Homogeneous, translucent, dark-greenish
WGF 4	2.4	7.49± 0.98	0.3897± 0.0027	62.46 ± 1.06	102.45± 1.77	Excelle nt	Homogeneous, translucent, dark-greenish
WGF 5	3.0	7.57± 0.99	0.3899± 0.0018	69.49 ± 1.12	100.00± 1.72	Excelle nt	Homogeneous, translucent, dark-greenish
WGF 6	3.6	7.37± 1.09	0.3902± 0.0020	75.73 ± 1.31	101.67± 1.91	Excelle nt	Homogeneous, translucent, dark-greenish

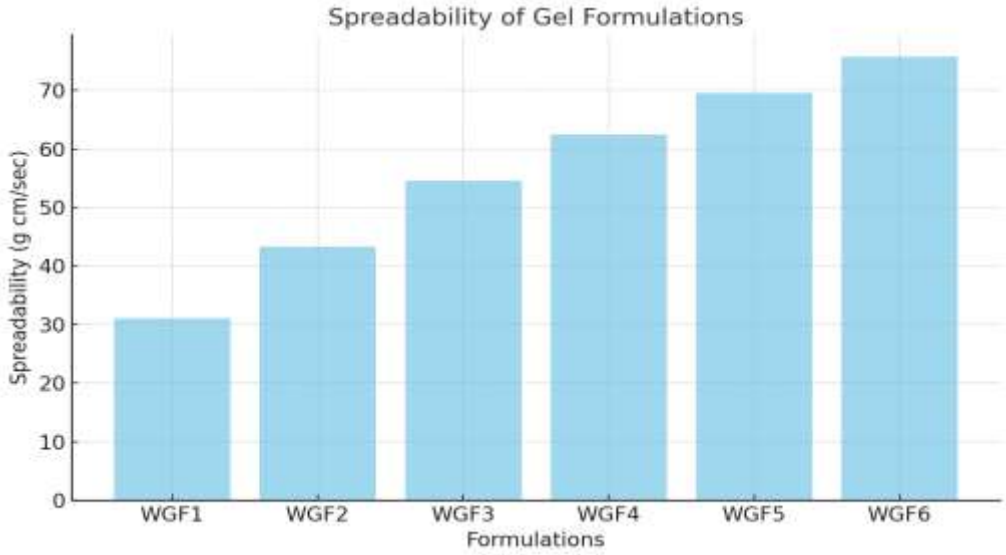

Figure 5. Spreadability of Gel Formulations

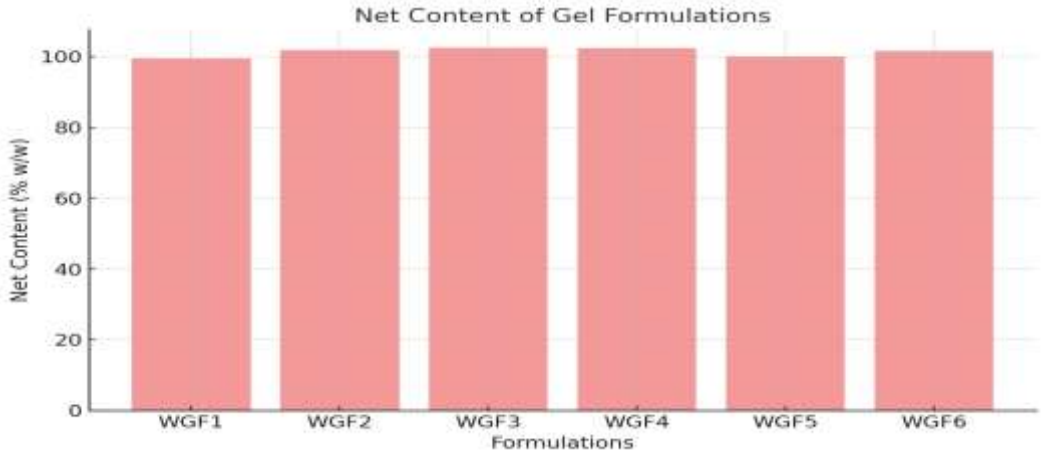

Figure 6. Net Content of Gel Formulations

In vitro diffusion profile and the drug release kinetics

The in vitro diffusion study of the gel formulations (WGF1 to WGF6) revealed a time-dependent release pattern of the active constituents, with variations observed based on the extract concentration in each formulation. The percentage cumulative drug release data, measured over a period of 5 hours, highlighted significant differences in diffusion profiles among the formulations. At the 1-hour mark, the percentage diffusion ranged from 8.37 ± 0.99% (WGF1) to 17.89 ± 0.99% (WGF2), indicating an initial burst release for higher extract concentrations. By the 2-hour mark, WGF2 showed the highest diffusion (34.49 ± 1.01%), while WGF1 exhibited a comparatively lower release (16.48 ± 0.98%). This trend persisted at the 3-hour mark, with WGF2 achieving 69.86 ± 1.03% release, significantly higher than WGF1 (32.74 ± 1.01%). As the study progressed, WGF4 demonstrated the most consistent and substantial release, achieving 98.90 ± 1.12% at the 5-hour mark. This was closely followed by WGF5 (83.89 ± 1.08%) and WGF6 (83.38 ± 1.12%). WGF1, with the lowest extract concentration, exhibited the slowest release, reaching 65.86 ± 1.09% by the end of the study. Notably, WGF2 showed a rapid release profile, achieving peak diffusion earlier than other formulations, indicating a potential for faster drug delivery. These findings suggest that higher concentrations of the active extract in the formulations (e.g., WGF4 to WGF6) supported sustained and controlled release, whereas lower concentrations (e.g., WGF1) resulted in slower diffusion. The release behavior can be attributed to the polymer matrix of Carbopol 934, which modulates the diffusion of the active constituents. Formulation WGF4, with its optimal balance

of extract concentration and gel matrix properties, demonstrated the most efficient release profile, making it a promising candidate for therapeutic applications requiring sustained drug delivery.

Table 6. *In vitro* diffusion profile

TIME (Hr)	**Gel Formulations**					
	WGF1	**WGF2**	**WGF3**	**WGF4**	**WGF5**	**WGF6**
1	8.37±0.99	17.89±0.99	10.76±0.98	17.76±1.00	11.39±0.99	13.87±1.07
2	16.48±0.98	34.49±1.01	24.93±0.99	33.65±1.01	26.54±0.99	27.48±1.08
3	32.74±1.01	69.86±1.03	47.95±1.05	52.82±1.01	50.57±1.06	55.47±1.11
4	41.45±1.02	89.85±1.10	63.68±1.08	69.75±1.06	67.88±1.07	65.56±1.09
5	65.86±1.09	79.79±1.08	78.88±1.09	98.90±1.12	83.89±1.08	83.38±1.12

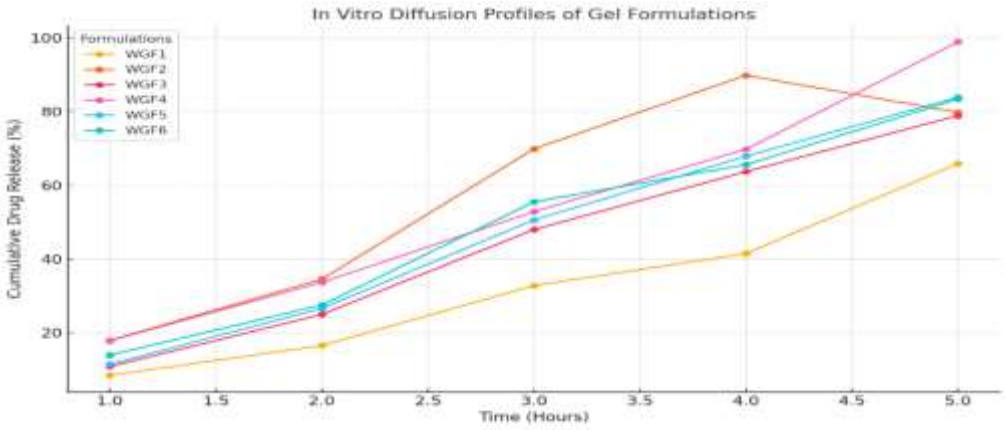

Figure 7. Diffusion profile of topical herbal gels *in vitro*.

Kinetic modelling of *In vitro* release data

The kinetic modelling of the in vitro release data for the gel formulations (WGF1 to WGF6) provided insights into their release mechanisms. The formulations were analyzed using Zero Order, First Order, and Higuchi Diffusion models, with the best-fitted model identified based on the highest R^2 values. WGF1 showed the strongest correlation with the First Order model (R2=0.9701), indicating a concentration-dependent release, where the release rate decreases as the concentration of the active ingredient diminishes. WGF2 aligned best with the Higuchi Diffusion model (R2=0.8876), suggesting a diffusion-controlled release governed by the concentration gradient of the active ingredient through the gel matrix.

In contrast, formulations WGF3, WGF4, WGF5, and WGF6 exhibited the best fit with the Zero Order model (R2=0.9941, R2=0.9860, R2=0.9947, and R2=0.9733, respectively), demonstrating a constant release rate over time, independent of the active ingredient concentration. This behaviour reflects a controlled and sustained release mechanism, which is ideal for achieving consistent therapeutic outcomes. The high correlation with the Zero Order model for these formulations highlights their suitability for applications requiring predictable and steady drug delivery. Overall, the modelling results reveal that the release mechanism varies with the concentration of the active ingredient and the gel matrix properties. While WGF1 and WGF2 exhibited concentration-dependent and diffusion-controlled releases, respectively, the majority of the formulations followed a Zero Order release pattern, underscoring their potential for delivering the active ingredient in a sustained and controlled manner. These findings provide a strong foundation for further development and optimization of the gel formulations for therapeutic (Kataki et al., 2017, Kataki et al., 2014, Kataki, 2010).

Table 7. Kinetic modelling of *In vitro* drug release data

Code for Formulations	Zero order	First Order	Higuchi diffusion model	Best fitted model
	R^2	R^2	R^2	
WGF1	0.9644	0.9701	0.9214	First Order
WGF2	0.8467	0.8343	0.8876	Higuchi Diffusion Model
WGF3	0.9941	0.9263	0.9843	Zero Order
WGF4	0.9860	0.9731	0.9524	Zero Order
WGF5	0.9947	0.9272	0.9843	Zero Order
WGF6	0.9733	0.9321	0.9457	Zero Order

4. Conclusion

The study successfully developed and characterized PHLE-MA-based herbal gel formulations, demonstrating their potential as effective topical therapeutic agents. The formulations showed desirable physicochemical properties, including optimal pH, viscosity, and spreadability, making them suitable for skin application. In vitro diffusion studies revealed a sustained release profile, particularly in formulations with higher extract concentrations, aligning with the Zero Order kinetic model. The significant lipid peroxidation inhibition observed in egg yolk and liver homogenate models highlighted the antioxidant efficacy of PHLE-MA. Moreover, COX inhibition studies confirmed its dual inhibitory activity against COX-1 and COX-2, emphasizing its anti-inflammatory potential. The total flavonoid content of PHLE-MA further validated its bioactivity, attributing its therapeutic properties to the high presence of phenolic compounds. Among the formulations, WGF4, WGF5, and WGF6 exhibited superior release profiles and sustained activity, indicating their suitability for prolonged therapeutic use. Overall, the study established PHLE-MA as a promising natural agent for topical applications, combining antioxidant and anti-inflammatory properties. These findings lay a robust foundation for future clinical investigations and the potential commercialization of PHLE-MA-based gel formulations for managing oxidative stress and inflammatory skin disorders.

DECLARATION OF INTEREST

None declared

FUNDING

Nil

5. References

1. AGUILAR, J. L., ROJAS, P., MARCELO, A., PLAZA, A., BAUER, R., REININGER, E., KLAAS, C. A. & MERFORT, I. 2002. Anti-inflammatory activity of two different extracts of *Uncaria tomentosa* (Rubiaceae) [J]. *Journal of Ethnopharmacology,* 81**,** 271-276.
2. AHMAD, S., ULLAH, F., ZEB, A., AYAZ, M., ULLAH, F. & SADIQ, A. 2016. Evaluation of Rumex hastatus D. Don for cytotoxic potential against HeLa and NIH/3T3 cell lines: chemical characterization of chloroform fraction and identification of bioactive compounds. *BMC Complement Altern Med,* 16**,** 308.
3. AIYALU, R., GOVINDARJAN, A. & RAMASAMY, A. 2016a. Formulation and evaluation of topical herbal gel for the treatment of arthritis in animal model. *Brazilian Journal of Pharmaceutical Sciences,* 52.
4. AIYALU, R., GOVINDARJAN, A. & RAMASAMY, A. 2016b. Formulation and evaluation of topical herbal gel for the treatment of arthritis in animal model. *Brazilian Journal of Pharmaceutical Sciences,* 52**,** 493-507.
5. BADMUS, J. A., ADEDOSU, T. O., FATOKI, J. O., ADEGBITE, V. A., ADARAMOYE, O. A. & ODUNOLA, O. A. 2011. Lipid Peroxidation Inhibition and Antiradical Activities of Some Leaf Fractions of *Mangifera Indica*. *Acta Poloniae Pharmaceutica - Drug Research,* 68**,** 23-29.
6. BLANCO-FUENTE, H., ANGUIANO-IGEA, S., OTERO-ESPINAR, F. J. & BLANCO-MÉNDEZ, J. 1996. In-vitro bioadhesion of carbopol hydrogels. *International journal of pharmaceutics,* 142**,** 169-174.

7. D'ABROSCA, B., CIARAMELLA, V., GRAZIANI, V., PAPACCIO, F., DELLA CORTE, C. M., POTENZA, N., FIORENTINO, A., CIARDIELLO, F. & MORGILLO, F. 2019. Urtica dioica L. inhibits proliferation and enhances cisplatin cytotoxicity in NSCLC cells via Endoplasmic Reticulum-stress mediated apoptosis. *Sci Rep,* 9**,** 4986.
8. GHASEMI, K., GHASEMI, Y. & EBRAHIMZADEH, M. A. 2009. Antioxidant activity, phenol and flavonoid contents of 13 citrus species peels and tissues. *Pak J Pharm Sci,* 22**,** 277-81.
9. GHASEMZADEH, A. & GHASEMZADEH, N. 2011. Flavonoids and phenolic acids: Role and biochemical activity in plants and human. *J. Med. Plants Res,* 5**,** 6697-6703.
10. HENDRIX, J., NIJS, J., ICKMANS, K., GODDERIS, L., GHOSH, M. & POLLI, A. 2020. The Interplay between Oxidative Stress, Exercise, and Pain in Health and Disease: Potential Role of Autonomic Regulation and Epigenetic Mechanisms. *Antioxidants (Basel, Switzerland),* 9**,** 1166.
11. HUQ, A., JAMAL, J. A., STANSLAS, J. J. E.-B. C. & MEDICINE, A. 2014. Ethnobotanical, phytochemical, pharmacological, and toxicological aspects of Persicaria hydropiper (L.) Delarbre. 2014.
12. JAIN, B. D. 2007. Formulation Development And Evaluation Of Fluconazole Gel In Various Polymer Basesformulation Development And Evaluation Of Fluconazole Gel In Various Polymer BaseS. *Asian Journal of Pharmaceutics (AJP),* 1.
13. KAKOTI, B. B., HERNANDEZ-ONTIVEROS, D. G., KATAKI, M. S., SHAH, K., PATHAK, Y. & PANGULURI, S. K. J. F. I. C. M. 2015. Resveratrol and omega-3 fatty acid: its implications in cardiovascular diseases. 2**,** 38.
14. KATAKI, M. S., KAKOTI, B. B., BHUYAN, B., RAJKUMARI, A. & RAJAK, P. J. C. J. O. N. M. 2014. Garden rue inhibits the arachidonic acid pathway, scavenges free radicals, and elevates FRAP: role in inflammation. 12**,** 172-179.
15. KATAKI, M. S., MURUGAMANI, V., RAJKUMARI, A., MEHRA, P., AWASTHI, D. & YADAV, R. S. 2012. Antioxidant, Hepatoprotective, and Anthelmintic Activities of Methanol Extract of Urtica dioica L. Leaves. *Pharmaceutical Crops,* 3**,** 38-46.
16. KATAKI, M. S., RAJKUMARI, A., MAZUMDER, B. J. N., RELEVANCE, N. C. & PREVENTION, D. 2017. Nutrition and Healthy Aging. 451.
17. KATAKI, M. S. J. P. O. 2010. Antibacterial activity, in vitro antioxidant activity and anthelmintic activity of ethanolic extract of Ananas comosus L. tender leaves. 2**,** 308-319.
18. KHARE, C. P. 2008. *Indian medicinal plants: an illustrated dictionary*, Springer Science & Business Media.
19. KOHLI, D. P. S. & SHAH, D. H. 1998. *Drug Formulations Manual*, Eastern Publishers.
20. LI, C., HUANG, Q., FU, X., YUE, X. J., LIU, R. H. & YOU, L. J. 2015. Characterization, antioxidant and immunomodulatory activities of polysaccharides from Prunella vulgaris Linn. *Int J Biol Macromol,* 75**,** 298-305.
21. LI, H.-L., LIU, D.-P. & LIANG, C.-C. 2003. Paraoxonase gene polymorphisms, oxidative stress, and diseases. *Journal of Molecular Medicine,* 81**,** 766-779.
22. LOGANATHAN, V., MANIMARAN, S., JASWANTH, A., SULAIMAN, A., REDDY, M. V. S., KUMAR, B. S. & RAJASESKARAN, A. 2001. The effects of polymers and permeation enhancers on releases of flurbiprofen from gel formulations. *Indian Journal of Pharmaceutical Sciences,* 63**,** 200.
23. MANDAL, V., MOHAN, Y. & HEMALATHA, S. 2007. Microwave assisted extraction—an innovative and promising extraction tool for medicinal plant research. *Pharmacognosy reviews,* 1**,** 7-18.
24. MARTIN, A. N., SINKO, P. J. & SINGH, Y. 2011. *Martin's Physical Pharmacy and Pharmaceutical Sciences: Physical Chemical and Biopharmaceutical Principles in the Pharmaceutical Sciences*, Lippincott Williams & Wilkins.
25. MURTHY, S. N. & SHIVAKUMAR, H. N. 2010. Topical and transdermal drug delivery. *Handbook of non-invasive drug delivery systems.* Elsevier.
26. NANDGUDE, T., THUBE, R., JAISWAL, N., DESHMUKH, P., CHATAP, V. & HIRE, N. 2008. Formulation and evaluation of pH induced in-situ nasal gel of salbutamol sulphate. *International Journal of Pharmaceutical Sciences and Nanotechnology (IJPSN),* 1**,** 177-183.

27. NAYAK, S. H., NAKHAT, P. D. & YEOLE, P. G. 2005. Development and evaluation of cosmeceutical hair styling gels of ketoconazole. *Indian journal of pharmaceutical sciences,* 67**,** 231.
28. OKTAY, A. N., ILBASMIS-TAMER, S., HAN, S., ULUDAG, O. & CELEBI, N. 2020. Preparation and in vitro/in vivo evaluation of flurbiprofen nanosuspension-based gel for dermal application. *European Journal of Pharmaceutical Sciences,* 155**,** 105548.
29. PACKER, L. 2001. *Handbook of Antioxidants,* Taylor & Francis.
30. PANIGRAHI, L., GHOSAL, S. K., PATTNAIK, S., MAHARANA, L. & BARIK, B. B. 2006. Effect of permeation enhancers on the release and permeation kinetics of lincomycin hydrochloride gel formulations through mouse skin. *Indian journal of pharmaceutical sciences,* 68.
31. QUEIROZ, M. B. R., MARCELINO, N. B., RIBEIRO, M. V., ESPINDOLA, L. S., CUNHA, F. R. & SILVA, M. V. D. 2009. Development of gel with Matricaria recutita L. extract for topic application and evaluation of physical-chemical stability and toxicity. *Lat. Am. J. Pharm,* 28**,** 574-579.
32. RATZ-ŁYKO, A., ARCT, J., MAJEWSKI, S. & PYTKOWSKA, K. 2015. Influence of polyphenols on the physiological processes in the skin. *Phytotherapy Research,* 29**,** 509-517.
33. RE, R., PELLEGRINI, N., PROTEGGENTE, A., PANNALA, A., YANG, M. & RICE-EVANS, C. 1998. Antioxidant activity applying an improved ABTS radical cation decolorization assay. *Free Radical Biology and Medicine,* 72**,** 1231-1237.
34. REDL, K., BREU, W., DAVIS, B. & BAUER, R. 1994. Anti-inflammatory active polyacetylenes from *Bidens campylotheca* [J]. *Planta Medica,* 60.
35. RUCH, R. J., CHENG, S. J. & KLAUNIG, J. E. 1989. Prevention of cytotoxicity and inhibition of intracellular communication by antioxidant catechins isolated from Chinese green tea. *Carcinogenesis,* 10**,** 1003-1008.
36. SEELINGER, G., MERFORT, I., WÖLFLE, U. & SCHEMPP, C. M. 2008. Anti-carcinogenic effects of the flavonoid luteolin. *Molecules,* 13**,** 2628-2651.
37. SOGA, M., MATSUZAWA, A. & ICHIJO, H. 2012. Oxidative Stress-Induced Diseases via the ASK1 Signaling Pathway. *International Journal of Cell Biology,* 2012**,** 439587.
38. SREEJAYAN, N. & RAO, M. N. A. 1997. Nitric oxide scavenging by curcuminoids. *J Pharm Pharmacol,* 49**,** 105-107.
39. STELMAKIENĖ, A., RAMANAUSKIENĖ, K. & BRIEDIS, V. 2015. Release of rosmarinic acid from semisolid formulations, and its penetration through the human skin ex vivo. *Acta Pharmaceutica,* 65**,** 199-205.
40. WALKER, R. B. & SMITH, E. W. 1996. The role of percutaneous penetration enhancers. *Advanced Drug Delivery Reviews,* 18**,** 295-301.
41. WU, Y., LI, L., WEN, T. & LI, Y.-Q. 2007. Protective effects of echinacoside on carbon tetrachloride-induced hepatotoxicity in rats. *Toxicology,* 232**,** 50-56.